Synthesis of TiO2–Poly(3-hexylthiophene) Hybrid Particles through Surface-Initiated Kumada Catalyst-Transfer Polycondensation

ARTICLE *in* LANGMUIR · SEPTEMBER 2014

Impact Factor: 4.46 · DOI: 10.1021/la502944g · Source: PubMed

9 AUTHORS, INCLUDING:

Yannick Guari
French National Centre for Scientific Research
131 PUBLICATIONS **2,476** CITATIONS
SEE PROFILE

Ahmad Mehdi
Université Montpellier
146 PUBLICATIONS **2,840** CITATIONS
SEE PROFILE

Philippe Dubois
Université de Mons
741 PUBLICATIONS **22,445** CITATIONS
SEE PROFILE

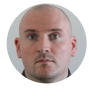

Sébastien Clément
Université de Montpellier
53 PUBLICATIONS **354** CITATIONS
SEE PROFILE

Langmuir

Article

pubs.acs.org/Langmuir

Synthesis of TiO_2–Poly(3-hexylthiophene) Hybrid Particles through Surface-Initiated Kumada Catalyst-Transfer Polycondensation

Florian Boon,[†,‡] David Moerman,[‡] Danielle Laurencin,[§] Sébastien Richeter,[§] Yannick Guari,[§] Ahmad Mehdi,[§] Philippe Dubois,[†] Roberto Lazzaroni,[‡] and Sébastien Clément*[,§]

[†]Laboratory of Polymeric and Composite Materials, Center of Innovation and Research in Materials and Polymers (CIRMAP), University of Mons UMONS, Place du Parc 20, 7000 Mons, Belgium

[‡]Laboratory for Chemistry of Novel Materials, CIRMAP, University of Mons UMONS, Place du Parc 20, 7000 Mons, Belgium

[§]Institut Charles Gerhardt Montpellier ICGM, UMR 5253, CNRS-UM2-ENSCM-UM1, Université Montpellier 2, Bâtiment 17, CC 1701 Place E. Bataillon, 34095 Montpellier Cedex 5, France

Supporting Information

ABSTRACT: TiO_2/conjugated polymers are promising materials in solar energy conversion where efficient photoinduced charge transfers are required. Here, a "grafting-from" approach for the synthesis of TiO_2 nanoparticles supported with conjugated polymer brushes is presented. Poly(3-hexylthiophene) (P3HT), a benchmark material for organic electronics, was selectively grown from TiO_2 nanoparticles by surface-initiated Kumada catalyst-transfer polycondensation. The grafting of the polymer onto the surface of the TiO_2 nanoparticles by this method was demonstrated by ^1H and ^{13}C solid-state NMR, X-ray photoelectron spectrometry, thermogravimetric analysis, transmission electron microscopy, and UV–visible spectroscopy. Sedimentation tests in tetrahydrofuran revealed improved dispersion stability for the TiO_2@P3HT hybrid material. Films were produced by solvent casting, and the quality of the dispersion of the modified TiO_2 nanoparticles was evaluated by atomic force microscopy. The dispersion of the P3HT-coated TiO_2 NPs in the P3HT matrix was found to be homogeneous, and the fibrillar structure of the P3HT matrix was maintained which is favorable for charge transport. Fluorescence quenching measurements on these hybrid materials in $CHCl_3$ indicated improved photoinduced electron-transfer efficiency. All in all, better physicochemical properties for P3HT/TiO_2 hybrid material were reached via the surface-initiated "grafted-from" approach compared to the "grafting-onto" approach.

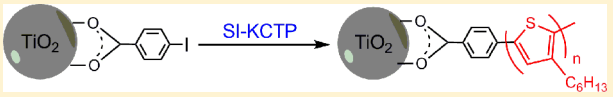

INTRODUCTION

Conjugated polymers (CPs) have attracted huge interest in recent years due to their applications in many optical and electronic devices such as organic light-emitting diodes (OLEDs),[1,2] field-effect transistors (FETs),[3,4] sensors[5] and polymer solar cells (PSCs).[6] A typical approach to fabricate PSCs is to employ the bulk-heterojunction (BHJ) concept where the photoactive layer is built upon an interpenetrating network of donor (conjugated polymer) and acceptor (mainly fullerene derivative) materials.[7] While the power conversion efficiency (PCE) of PSCs has increased recently to over 8% in single BHJ PSCs,[8] their instability, particularly in the presence of oxygen and moisture, as well as the poor electron mobility of fullerene derivatives are critical issues for the cell performance and lifetime.[9]

An alternative to fully organic BHJ consists of combining conjugated polymers with *n*-type inorganic semiconductors.[10,11] These {conjugated polymers}/{inorganic semiconductor} hybrid materials can take benefit from the properties of both types of materials: easy solution processing of the CPs on one hand, and higher thermal and ambient stabilities and higher electron mobility of the inorganic semiconductors on the other. So far, various hybrid polymer solar cells including inorganic semiconductors such as TiO_2,[12,13] ZnO,[14,15] CdSe,[16] and PbS[17] have been reported. Among these, titanium dioxide is one of the most widely studied phases due to its lack of toxicity, its relatively low cost of production, and its tunable morphology, as it can be fabricated in various sizes and shapes, including spheres, tubes, and rods. The possibility to tailor the dimensionality and morphology of TiO_2 particles offers the opportunity to optimize the charge transport in the photovoltaic device.[18] For example, Chen *et al.* demonstrated that the dimensionality and anisotropy of TiO_2 nanocrystals in P3HT:TiO_2 (P3HT = poly(3-hexylthiophene)) hybrids could lead to carrier transport behaviors in directions perpendicular or parallel to the film substrate, when switching from nanorods to nanospheres.[19] Another critical issue of these organic–inorganic hybrids is the inherent incompatibility between the hydrophilic surface of the metal oxide and the hydrophobic nature of the conjugated polymers, which frequently triggers phase segregation between the electron donor and acceptor components, leading to reduced carrier-dissociation efficiency.[20] Thus, improving the miscibility and dispersion

Received: July 25, 2014
Revised: September 4, 2014
Published: September 4, 2014

dx.doi.org/10.1021/la502944g | *Langmuir* 2014, 30, 11340–11347

Scheme 1. Preparation of Poly(3-hexylthiophene) Brushes by a "Grafting-from" Strategy Followed by Polymer-Analogous Transformations (COD = 1,5-cyclooctadiene; bpy = 2,2′-bipyridine)

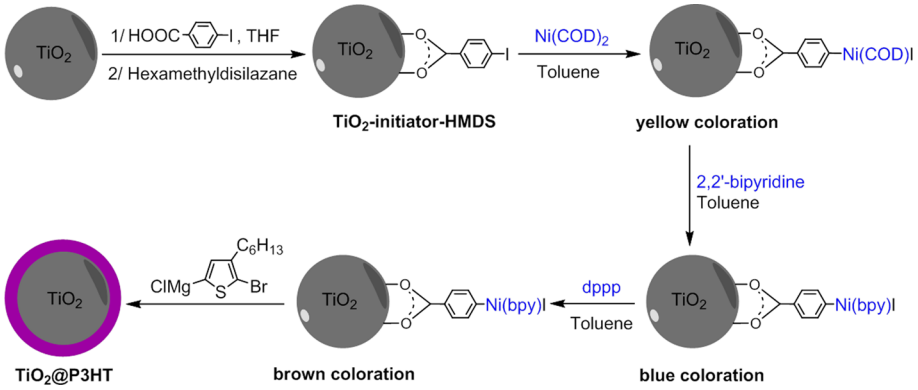

stability of CP:TiO_2 hybrids, while maintaining good electron-transfer properties is crucial.

Inorganic semiconductors used in hybrid solar cells are in general prepared by colloidal synthesis, leading to the formation of nanocrystals (NCs) whose size and shape are determined by the nature of the surface organic ligands chosen (alkyl thiols, amines, phosphines, and phosphine oxides) and the temperature.[21,22] The organic molecules on the surface of the inorganic semiconductor NCs ensure their dispersion in solution and miscibility in the polymer matrix. However, the insulating nature of these ligands severely affects the morphology of NC:CP films and reduces the charge transfer operating between CPs and NCs, as well as the electron transport between NCs.[21,22]

One of the most promising alternatives to significantly increase both miscibility and electrical performance is to directly modify the surface of the inorganic semiconductors with CPs.[10] In principle, three different approaches exist for the modification of the surface of the inorganic semiconductors with CP chains. In "grafting-onto" approaches, CP contains a functional group at one chain end, obtained either from the polymerization technique or by postpolymerization chemical transformations. This end group is then reacted with a complementary functional group on the NC surface.[23] This approach has the advantage of simplicity, but usually results in low grafting density of the polymer; the grafting being limited both thermodynamically and kinetically. For example, we have recently reported the grafting of a carboxylic end-functionalized P3HT onto the surface of TiO_2 nanoparticles (leading to improved photoinduced electron-transfer efficiency),[24] in which only 3% of this polymer was grafted to TiO_2. Another straightforward technique is the "grafting-through" approach, which consists of performing a solution polymerization in the presence of a material whose surface is functionalized with groups which are reactive in the polymerization. Unfortunately, as in the case of the grafting-onto approach, this strategy is intrinsically limited to low grafting densities and low layer thicknesses.[25]

The third approach, referred to as the "grafting-from" approach is based on the immobilization of an initiator at the surface of a material, followed by the reaction of this surface-bound species with monomers in solution. Compared to grafting-onto and grafting-through strategies, the packing density of grafted polymers as well as the nature of the immobilized chains can be more carefully controlled.[26,27] Indeed, if the initiation is efficient and if the polymerization follows a chain-growth mechanism, stretched polymer chains with high molecular weights (exceeding 10^6 g mol^{-1}) and low polydispersity (<1.5), can be covalently immobilized at the surface of a substrate with a high density. Approximately 10 years ago, the groups of Yokozawa[28] and McCullough[29] independently reported that P3HT with controlled molecular weight and narrow molecular weight distribution could be synthesized by using a Kumada catalyst-transfer polycondensation (KCTP) polymerization. Since then, other well-defined conjugated polymers such as polyfluorenes,[30] polypyrroles,[31] and poly(carbazoles)[32] as well as all-conjugated block copolymers have been synthesized using KCTP.[33,34] It was clearly established that this polymerization follows a chain-growth mechanism rather than a step-growth one, opening the door to the growth of conjugated polymer brushes on organic or inorganic surfaces via the grafting-from approach. Kiriy et al. reported the first preparation of P3HT brushes from immobilized polystyrene[35,36] or silica particles[37] via the surface-initiated Kumada catalyst-transfer polycondensation (SI-KCTP). Since then, several conjugated polymers such as polyfluorenes and poly(dialkoxy-*p*-phenylenes) have been synthesized using KCTP from initiators that are covalently bonded to silica, indium tin oxide, or polystyrene.[26,27,38]

Herein, based on this strategy, we report the synthesis of TiO_2@P3HT hybrid nanoparticles (NPs) through SI-KCTP. P3HT was selectively grown from TiO_2 NPs modified with 4-iodobenzoic acid initiator. The hybrid materials were thoroughly characterized to evidence the presence of a P3HT layer onto the TiO_2 NPs and to demonstrate the different steps of the grafting procedure, using solid-state nuclear magnetic resonance (NMR) and X-ray photoelectron spectroscopy (XPS). Finally, some preliminary properties such as the dispersion stability and the photoinduced electron-transfer efficiency were studied to assess the potential of this material for use in hybrid photovoltaic devices.

RESULTS AND DISCUSSION

The general strategy we used to prepare TiO_2@P3HT hybrids using a grafting-from approach is shown in Scheme 1. To apply the SI-KCTP technique to TiO_2 NPs, 4-iodobenzoic acid was used as the anchoring initiator. It was grafted onto the surface of the TiO_2 NPs through Ti−O−C bonds by treatment of TiO_2 NPs with a solution of 4-iodobenzoic acid in tetrahydrofuran (THF).

The success of this grafting was attested to by ^{1}H and ^{13}C solid-state NMR (Figure 1, green spectra). Indeed, signals

dx.doi.org/10.1021/la502944g | Langmuir 2014, 30, 11340−11347

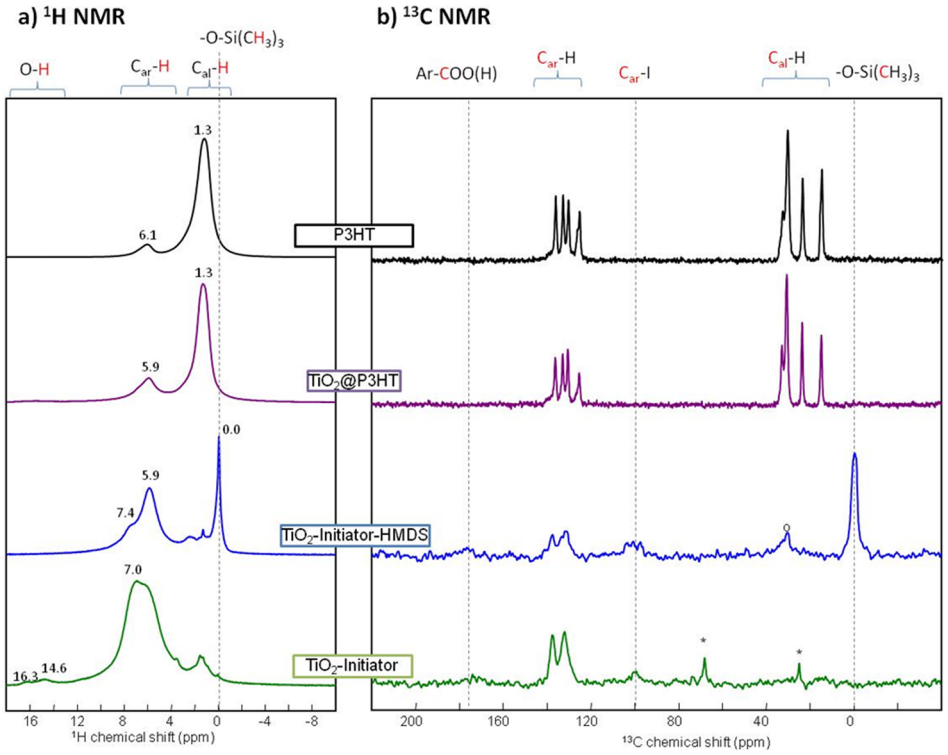

Figure 1. (a) ^{1}H MAS solid-state NMR and (b) ^{13}C CP MAS solid-state NMR of TiO_2-grafted with the initiator (green), TiO_2-grafted with the initiator and protected with HMDS (blue), TiO_2@P3HT hybrid material (purple), and pristine P3HT (black) (* and O are residual impurities in the rotor).

corresponding to the aromatic ring are clearly visible on both spectra: at ∼7 ppm (^{1}H NMR) and between 125 and 140 ppm (^{13}C NMR). The signals of the carboxylic group anchored on the TiO_2 surface (at ∼175 ppm) and of the C atom directly bound to the iodine (at ∼100 ppm) are significantly broadened, due to the surface binding in the former case,[39] and due to residual dipolar coupling to the quadrupolar ^{127}I nucleus in the latter case.[40] It is worth noting that the ^{1}H NMR spectra also show the presence of H-bonded O−H groups (peaks between 14 and 17 ppm), which could belong to residual -COOH groups, or to Ti−OH surface functions. Other weak resonances between 0 and 8 ppm may correspond to other types of surface hydroxyl groups.

Prior to the insertion of the nickel catalyst and surface-initiated polymerization, all of the hydroxyl functions available on the TiO_2 surface needed to be "masked" in order to avoid side reactions with 2-bromo-5-chloromagnesio-3-hexylthiophene. Thus, a treatment with hexamethyldisilazane (HMDS) was performed, in order to protect the hydroxyl functions with a trimethylsilyl group. The resulting product was characterized by ^{1}H and ^{13}C solid-state NMR (Figure 1, blue spectra). As expected, strong signals characteristic of the trimethylsilyl groups are observed on the ^{1}H and ^{13}C NMR spectra, with sharp peaks centered at 0 ppm in ^{1}H and ^{13}C NMR. The high-frequency ^{1}H signals corresponding to O−H groups have disappeared, confirming the efficiency of the HMDS treatment. The changes observed on the ^{1}H NMR spectrum between 2 and 8 ppm may also be due to the removal of other types of Ti−OH groups from the surface (whose ^{1}H NMR signals previously overlapped with the aromatic proton signatures). The XPS spectrum of TiO_2-initiator-HMDS (Figures S1 and S2 in the Supporting Information) shows the presence of Ti, O, C, I, and Si confirming the grafting of 4-iodobenzoic acid onto the TiO_2 surface and the passivation of the surface with HMDS.

Once all of the hydroxyl groups had been protected with HMDS, the catalyst necessary for chain-growth SI-KCTP was immobilized by following the procedure described in Scheme 1. Since the traditional catalyst used in KCTP ($Ni(dppp)Cl_2$) (dppp = bis(diphenylphosphino)propane) had been shown to be unreactive toward unactivated arylhalides,[41] a Ni(0) species ($Ni(COD)_2$) was chosen instead. Then, additional exchange reactions with bpy and phosphine ligand were performed to obtain the bound-Ni(dppp) catalyst.[42] Indeed, it had been shown that by using this supplementary ligand exchange from COD to bpy before the final exchange with dppp, the homogeneity and the surface coverage of the final Ni(II) species could increase significantly (by 20%).[43] The functionalized NPs were then isolated and carefully purified to remove physisorbed Ni.

To perform SI-KCTP, 2-bromo-5-chloromagnesio-3-hexylthiophene was added to the dispersion of the activated NPs, and the polymerization was then performed during 2 days, after which the reaction was quenched by adding 5 M HCl. The functionalized nanoparticles were separated by centrifugation, isolated as a purple powder (TiO_2@P3HT), purified by washing, and properly dried prior to any further characterization.

Solid-state NMR analyses were then performed on the TiO_2@P3HT hybrid material and compared to pure P3HT (Figure 1, purple spectra). The ^{1}H MAS NMR spectrum of the TiO_2@P3HT hybrid material (Figure 1a) exhibited two main peaks centered at 1.3 and 5.9 ppm. These are characteristic of the alkyl protons of the C_6H_{13} side chains and of the thiophene protons of P3HT, as it appears on the ^{1}H solid-state NMR spectrum of pristine P3HT (Figure 1a, black spectrum). It is

dx.doi.org/10.1021/la502944g | Langmuir 2014, 30, 11340−11347

worth noting however that the chemical shift of the thiophene proton in solid-state NMR is quite different from that measured in solution (~7 ppm), suggesting that chain planarization and $\pi-\pi$ stacking interactions most probably occur between the P3HT chains grafted onto the TiO_2 surface. This is also consistent with the fact that, in the solid, the hybrid material is purple, which is typical of aggregated, interacting P3HT chains, rather than orange (typical of solvated, coiled chains).[44] In the ^{13}C CP MAS NMR (Figure 1b), the similarity between the spectra of TiO_2@ P3HT and pristine P3HT is also observed: in both cases, the spectrum reveals the presence of four aromatic peaks above 120 ppm corresponding to the four aromatic carbon atoms of the thiophene unit,[45,46] two aliphatic peaks for the methyl and methylene groups (18 and 22 ppm) and other aliphatic signals around 30 ppm corresponding to the inner methylene groups.[47] Signals characteristic of the trimethylsilyl groups on the ^1H and ^{13}C NMR spectra are no longer observed indicating the desilylation and the re-formation of the Ti−OH groups after the acid quenching of the polymerization. This finding was confirmed by the absence of a peak corresponding to Si in the XPS spectrum of the TiO_2@P3HT hybrid material (Figure S3 in the Supporting Information). In comparison to the TiO_2-initiator-HMDS hybrid material, two peaks in the O(1s) orbital spectrum of the TiO_2@P3HT hybrid material at binding energies of 530.0 and 532.0 eV were noticed (Figure S4 in the Supporting Information). The peak at higher binding energy may be attributed to Ti−OH groups re-formed on the TiO_2 surface after the acid quenching of the polymerization.

To study the influence of the P3HT shell on the dispersion stability of the functionalized TiO_2 particles, the neat and TiO_2@P3HT NPs (5 mg) were dispersed in THF (2 mL) by ultrasonication during 30 min. The sedimentation was followed visually. After 1 h, the neat TiO_2 particles were aggregated and left a clear supernatant. In contrast, the presence of the P3HT on the TiO_2 surface significantly improved the dispersion stability of TiO_2 in THF since the TiO_2@P3HT grafted NPs remain dispersed even after 24 h (Figure S5 in the Supporting Information). If we compare these results with those previously obtained for a P3HT-COOH/TiO_2 hybrid material using the grafting-onto approach,[24] a higher dispersion stability is noticed for TiO_2@P3HT NPs which may indicate a higher P3HT grafting density.

In order to quantify the amount of P3HT in TiO_2@P3HT NPs and also, to examine the degradation of the TiO_2@P3HT NPs upon thermal treatment, thermogravimetric analyses (TGA) were performed on the TiO_2@P3HT hybrid material (Figure 2). TGA were also performed on the TiO_2 particles grafted with the precursor (after masking of the surface Ti−OH functions), and on the neat TiO_2 NPs and P3HT, taken separately. The neat TiO_2 NPs showed only a very small weight loss (about 2 wt %) between 50 and 800 °C, while for pristine P3HT, a weight loss of about 70% was observed between 400 and 600 °C (data not shown).[14] For the TiO_2 nanoparticles grafted with the precursor (Figure 2), we can estimate from the TGA analysis that 1.5 wt % of the organic precursor has been grafted (4-iodobenzoic acid + trimethylsilyl). Thus, the amount of P3HT in the TiO_2@P3HT hybrid material was calculated to represent 13 wt %, based on the residual mass at 600 °C, and the following formula.

$$\text{wt \% P3HT} = \frac{(\text{wt loss } TiO_2\text{@P3HT} - \text{wt loss } TiO_2 - \text{initiator} - \text{HMDS})}{\text{wt loss pristine P3HT}} \times 100$$

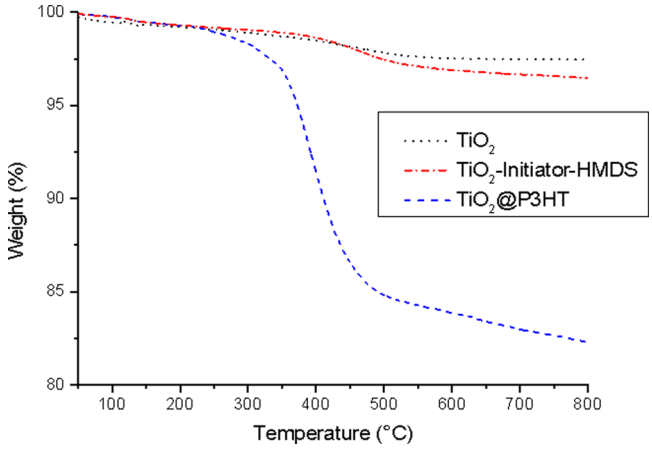

Figure 2. TGA diagrams for TiO_2 (Degussa P-25), TiO_2-initiator-HMDS and TiO_2@P3HT hybrid material.

As expected, compared to the grafting-onto strategy,[24] for which the weight percent of P3HT achieved was 3%, a much higher content of P3HT grafted on the TiO_2 surface was found with the grafting-from strategy, showing the clear advantage of the latter strategy.

The optical properties of the hybrid material were then analyzed by UV−vis spectroscopy (Figure 3). The spectrum of

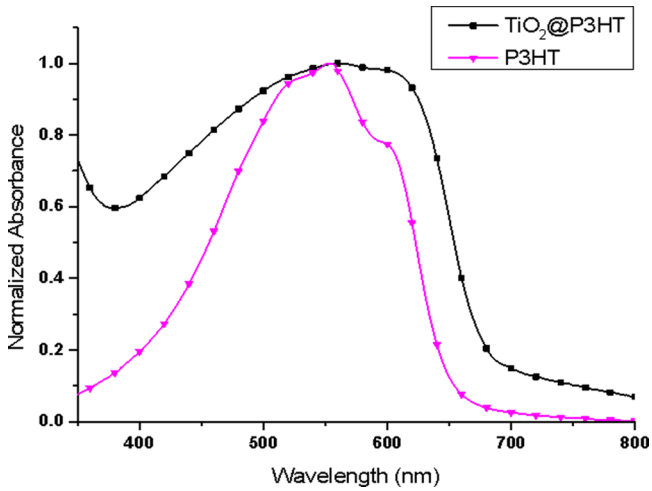

Figure 3. UV−vis absorption spectra of P3HT and TiO_2@P3HT hybrid material deposited on a quartz substrate.

P3HT in the solid state was recorded for comparison. As previously reported, the P3HT spectrum displays a bathochromic shift of the absorption maximum attributed to the $\pi-\pi^*$ transition in the polymer main chain at 550 nm as well as a vibrational structure.[44] The presence of a shoulder at about 620 nm is assigned to the vibronic progression of the C=C stretching mode ($\Delta E \approx 0.15$ eV).[47] Compared to pure P3HT, the spectrum of the TiO_2@P3HT hybrid material in the solid state also showed a broad absorption band centered at 550 nm, but a less pronounced vibronic structure was observed indicating a lower degree of chain planarization and ordering between the grafted chains in the hybrid material (Figure 3). The absorption of the composite for wavelengths lower than 400 nm is also increased due to the UV absorption of TiO_2. The high degree of scattering in the TiO_2@P3HT hybrid

dx.doi.org/10.1021/la502944g | Langmuir 2014, 30, 11340−11347

material leads to a shift of the baseline in the absorption spectrum of the composite.[48]

Transmission electron microscopy (TEM) was used to determine the thickness of the grafted P3HT layer on the TiO_2 surface. Figure 4 shows the core−shell TiO_2@P3HT NPs

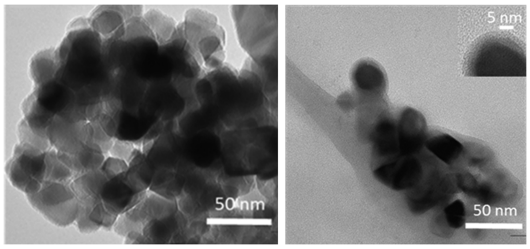

Figure 4. TEM images of TiO_2-initiator-HMDS (left) and TiO_2@P3HT nanoparticles (right).

indicating the presence of a homogeneous polymer shell around the TiO_2 NPs. The P3HT shell thickness in TiO_2@P3HT hybrid material ranges from 5 to 7 nm as estimated from TEM images. In the literature, a lamellar chain packing oriented parallel to the surface has been reported when amino-, triethoxysilane- and phosphonic ester-terminated P3HT are grafted onto ZnO nanowires, and this was explained by a chain folding.[14,15,49] Using the unit cell parameter of the P3HT (a = 16.2 Å, b = 3.8 Å, and c = 7.8 Å),[50,51] the average molecular weight, and the chemical repeat unit of P3HT, the length of the P3HT chain was then estimated and the shell thickness was explained based on the lamellar repeat folding (along the c-axis of the chain). Thus, for example, Fréchet *et al.* estimated a shell tichness of about 6−11 nm for a ∼7 kDa phosphonic ester-terminated P3HT.[15] If we follow these calculations, the average molecular weight of our P3HT would be between 3 and 5 kDa which is consistent with a shell thickness of 5−7 nm.

Atomic force microscopy (AFM) analysis was then performed on thin films of the TiO_2@P3HT hybrid particles (∼50 nm). The films were prepared from a mixture of P3HT:TiO_2@P3HT (1:1 in weight) deposited by drop casting of a 0.01 mg·mL^{-1} chlorobenzene solution on a glass substrate. Figure 5 shows that the dispersion of the P3HT-coated TiO_2

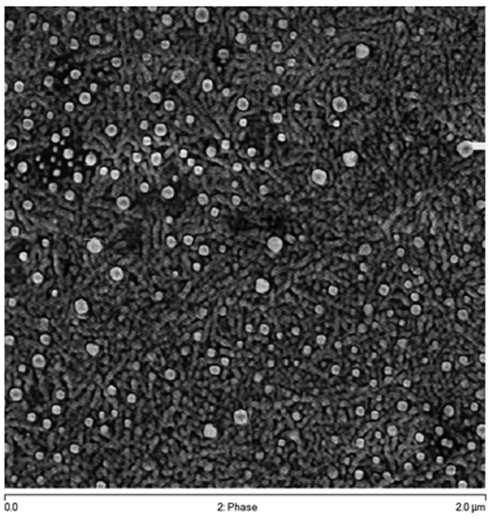

Figure 5. Tapping-mode AFM phase image (2 × 2 μm^2) of a thin deposit of 1:1 P3HT:TiO_2@P3HT in weight.

NPs in the P3HT matrix is homogeneous. This can be explained by the presence on the surface of the NPs of covalently grafted P3HT: the polymer shell reduces the interactions between the NPs and favors interactions with the polymer matrix. As a result, the NPs appear to be well-dispersed. The low content of NPs visible in the AFM images is consistent with the composition of the starting solution and the difference of material density: ∼1 for P3HT vs ∼4 for TiO_2. In the absence of the grafted polymer, the TiO_2 nanoparticles showed absolutely no capacity of dispersion in the P3HT films. It is also important to notice that contrary to the P3HT−COOH/TiO_2 hybrid material prepared from the grafting-onto approach,[24] the P3HT matrix keeps its fibrillar structure, which is favorable for charge transport.

To examine the efficiency of the photoinduced electron transfer across the donor−acceptor junction in the TiO_2@P3HT hybrid material, the photoluminescence (PL) spectrum of the TiO_2@P3HT hybrid material in $CHCl_3$ with an excitation wavelength of 440 nm was recorded and compared to the pristine P3HT and a physically mixed P3HT/TiO_2 hybrid (Figure 6). To compare the three materials, the P3HT

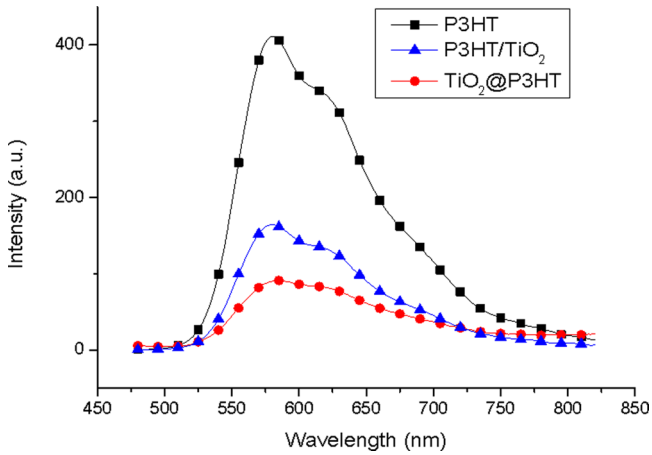

Figure 6. Emission spectra of P3HT, P3HT/TiO_2, and TiO_2@P3HT in $CHCl_3$ (λ_{ex} = 440 nm).

concentration was kept the same in the three samples: a concentration of 10^{-7} g·mL^{-1} was used, taking into account the P3HT covalently grafted on the NPs. If the TiO_2 can act as an electron acceptor when blended with P3HT, the electron transfer from the conjugated polymer to the titania matrix should result in the quenching of the P3HT fluorescence.[52] As shown in Figure 6, a significant quenching of the fluorescence in the composites was observed, when comparing to the pristine P3HT. The PL was quenched by a factor of about 2.5 in the case of physically blended P3HT/TiO_2 and about 5 for the TiO_2@P3HT hybrid material. The increased fluorescence quenching for TiO_2@P3HT hybrid material can be explained by the presence of the carboxylic group conjugated to the polymer skeleton which increases the interactions at the interface with the titanium oxide and thus, improves the photoinduced charge-transfer efficiency operating between the electron donor (P3HT) and the electron acceptor (TiO_2).[53−55]

CONCLUSION

An approach to synthesize TiO_2 nanoparticles-supported conjugated polymer brushes was described. Poly(3-hexylthiophene) was selectively grafted from TiO_2 nanoparticles by

dx.doi.org/10.1021/la502944g | *Langmuir* 2014, 30, 11340−11347

surface-initiated Kumada catalyst-transfer polycondensation. The anchoring of the polymer was demonstrated by sedimentation tests in THF and by thermogravimetric analysis, transmission electron microscopy, ^{1}H and ^{13}C MAS solid-state NMR, XPS, and UV−vis spectroscopies. By using this strategy, a higher P3HT grafting density and thus, a higher dispersion stability were obtained compared to the grafting-onto approach.[24] A 13 wt % amount of P3HT was grafted on TiO_2 NPs as evidenced by TGA analysis. $\pi-\pi$ stacking interactions between the grafted polymer chains in the hybrid material in the solid state for the nanohybrid materials were evidenced by the shielded chemical shift of the thiophene protons in ^{1}H MAS solid-state NMR spectroscopy and by the presence of a weak vibronic structure in the UV−vis spectrum.

AFM measurements performed on thin films of P3HT:TiO_2@P3HT (1:1 in weight) hybrid material showed a uniform dispersion of the TiO_2 NPs in the P3HT matrix. It is important to note that contrary to the P3HT−COOH/TiO_2 hybrid material prepared from the grafting-onto approach, the P3HT matrix keeps its fibrillar structure, which is favorable for charge transport. An improved photoinduced electron-transfer efficiency was also observed in the nanohybrid materials compared to a simple mixture of P3HT/TiO_2, due to the intimate contact between P3HT and the TiO_2 surface via the carboxylate group. Further work will build on the insights gained from this study to fabricate optimized hybrid polymer devices.

EXPERIMENTAL SECTION

Materials. All reactions were carried out under argon using standard high-vacuum and Schlenk techniques. 2-Bromo-3-hexyl-5-iodothiophene (BI3HT) was prepared according to literature methods.[56] *i*PrMgCl (2 M solution in THF) was purchased from Acros. 4-Iodobenzoic acid (98%), 1,3-bis(diphenylphosphino)propane (dppp; 97%), 2,2′-bipyridyl (99%), bis(1,5-cyclooctadiene)nickel(0) (Ni(COD)$_2$), and hexamethyldisilazane (99.9%) were purchased from Aldrich and were used as received without further purification. Dry THF was obtained by distillation first over CaH_2 and then sodium/benzophenone. Dry chloroform and chlorobenzene were obtained by distillation over P_2O_5. The TiO_2 nanoparticles used (P25 Degussa) were purchased from Degussa and were found to have an average particle diameter of 21 nm, a specific surface area of 45 ± 5 $m^2 \cdot g^{-1}$, and a density of 4.26. They contain anatase and rutile phases in a ratio of about 3, and their isoelectric point occurs at pH of about 5.8.[57]

Preparation of the TiO_2-Anchored Initiator. TiO_2 (1.00 g, Degussa P25) was suspended in 50 mL of THF. 4-Iodobenzoic acid (0.19 g, 0.75 mmol) was added, and the mixture was stirred for 48 h at room temperature. Then, the mixture was centrifuged. The residue was washed with 10 mL of THF and centrifuged again. This operation was repeated 3 times. The product was finally dried under vacuum for 3 h.

Passivation of the Residual Ti−OH in TiO_2-Anchored Initiator. In a round-bottom flask under argon, TiO_2-anchored initiator (500 mg) was suspended in 50 mL of dry toluene. To this suspension, hexamethyldisilazane (10 mL, 48 mmol) was added and the mixture was refluxed overnight. After cooling to room temperature, the mixture was centrifuged and the supernatant was removed. The residue was washed 2 times with dry THF and dried under vacuum. The product was then kept under nitrogen.

Preparation of the TiO_2@P3HT Hybrid Material. In a round-bottom flask under argon, the protected TiO_2-anchored initiator particles (400 mg) were suspended in 20 mL of dry THF, and Ni(COD)$_2$ (30 mg, 0.11 mmol) was added. The solution turned yellow, and the mixture was stirred for 2 h at room temperature. Then, 2,2′-bipyridine (18 mg, 0.11 mmol) was added, and the solution turned blue. After 2 h of stirring, dppp (45 mg, 0.11 mmol) was added and the solution turned brown. The suspension was allowed to react overnight. Prior to the surface-initiated polymerization, the suspension of the activated TiO_2 particles was cooled to 0 °C and decanted. The supernatant was removed under nitrogen. Several centrifugation/re-dispersion cycles were performed, centrifuging at 4000 rpm for 10 min, and using anhydrous and degassed THF in argon atmosphere, up until the supernatant solution remained colorless. In separate flask, BI3HT (0.75 g, 2 mmol) was dissolved in 10 mL of THF, 1 mL of *i*PrMgCl (2 M solution, 2 mmol) was added via a syringe, and the mixture was stirred at 0 °C for 30 min. To perform surface-initiated polymerization, the 2-bromo-5-chloromagnesio-3-hexylthiophene solution was transferred to the dispersion of the activated TiO_2 particles in 10 mL of THF, and the polymerization was carried out at room temperature for 48 h. After the polymerization, the resulting hybrid particles were carefully purified to separate any ungrafted polymers, catalyst, and byproducts. A typical purification procedure included several centrifugation/re-dispersion cycles, by successively adding 5 M HCl aqueous solutions, water, methanol, and $CHCl_3$.

ASSOCIATED CONTENT

Supporting Information

Text describing materials and characterization methods and figures showing XPS spectra of the TiO_2-initiator-HMDS and TiO_2@P3HT hybrid materials (wide scan) , of the I(3d5) core level of TiO_2-initiator-HMDS hybrid material, of the O(1s) core level of the TiO_2@P3HT and TiO_2-initiator-HMDS hybrid materials, and sedimentation tests in THF. This material is available free of charge via the Internet at http://pubs.acs.org.

AUTHOR INFORMATION

Corresponding Author

*E-mail: sebastien.clement02@univ-montp2.fr.

Notes

The authors declare no competing financial interest.

ACKNOWLEDGMENTS

We thank the CNRS and the Université Montpellier II for financial support. Research at CIRMAP is supported by the European Commission and Région Wallonne FEDER program, the Belgian Federal Government Office of Science Policy (Grant PAI 7/05), FNRS, and the OPTI^{2}MAT Excellence Program of Région Wallonne. F.B. and D.M. are grateful to FRIA for a doctoral grant.

REFERENCES

(1) Zucchi, G.; Tondelier, D.; Bonnassieux, Y.; Geffroy, B. Improving the performance of polymer light-emitting devices with chemical tools. *Polym. Int.* **2014**, *63* (8), 1368−1377.

(2) Kuik, M.; Wetzelaer, G.-J. A. H.; Nicolai, H. T.; Craciun, N. I.; De Leeuw, D. M.; Blom, P. W. M. Charge Transport and Recombination in Polymer Light-Emitting Diodes. *Adv. Mater.* **2014**, *26* (4), 512−531.

(3) Guo, X.; Baumgarten, M.; Muellen, K. Designing π-conjugated polymers for organic electronics. *Prog. Polym. Sci.* **2013**, *38* (12), 1832−1908.

(4) Lu, K.; Liu, Y. Polythiophenes: Important conjugated semiconducting polymers for organic field-effect transistors. *Curr. Org. Chem.* **2010**, *14* (18), 2017−2033.

(5) Rochat, S.; Swager, T. M. Conjugated Amplifying Polymers for Optical Sensing Applications. *ACS Appl. Mater. Interfaces* **2013**, *5* (11), 4488−4502.

(6) Li, G.; Zhu, R.; Yang, Y. Polymer solar cells. *Nat. Photonics* **2012**, *6* (3), 153−161.

(7) Nelson, J. Polymer: Fullerene bulk heterojunction solar cells. *Mater. Today* **2011**, *14* (10), 462−470.

(8) Umeyama, T.; Imahori, H. Design and control of organic semiconductors and their nanostructures for polymer-fullerene-based

photovoltaic devices. *J. Mater. Chem. A* **2014**, *2* (30), 11545−11560 and references therein.
(9) Krebs, F. C. Air stable polymer photovoltaics based on a process free from vacuum steps and fullerenes. *Sol. Energy Mater. Sol. Cells* **2008**, *92* (7), 715−726.
(10) Bousquet, A.; Awada, H.; Hiorns, R. C.; Dargon-Lartigau, C.; Billon, L. Conjugated-polymer grafting on inorganic and organic substrates: A new trend in organic electronic materials. *Prog. Polym. Sci.* **2014**, in press, DOI: 10.1016/j.progpolymsci.2014.03.003.
(11) Bouclé, J.; Ackermann, J. Solid-state dye-sensitized and bulk heterojunction solar cells using TiO_2 and ZnO nanostructures: recent progress and new concepts at the borderline. *Polym. Int.* **2012**, *61* (3), 355−373.
(12) Liao, W.-P.; Hsu, S.-C.; Lin, W.-H.; Wu, J.-J. Hierarchical TiO_2 Nanostructured Array/P3HT Hybrid Solar Cells with Interfacial Modification. *J. Phys. Chem. C* **2012**, *116* (30), 15938−15945.
(13) Thalluri, G. K. V. V; Bolsée, J.-C.; Gadisa, A.; Parchine, M.; Boonen, T.; D'Haen, J.; Boyukbayram, A. E.; Vandenbergh, J.; Cleij, T. J.; Lutsen, L.; Vanderzande, D.; Manca, J. Opto-electrical and morphological characterization of water soluble conjugated polymers for eco-friendly hybrid solar cells. *Sol. Energy Mater. Sol. Cells* **2011**, *95*, 3262−3268.
(14) Awada, H.; Medlej, H.; Blanc, S.; Deville, M.-H.; Hiorns, R. C.; Bousquet, A.; Dagron-Lartigau, C.; Billon, L. Versatile functional poly(3-hexylthiophene) for hybrid particles synthesis by the grafting onto technique: Core@shell ZnO nanorods. *J. Polym. Sci., Part A: Polym. Chem.* **2014**, *52* (1), 30−38.
(15) Briseno, A. L.; Holcombe, T. W.; Boukai, A. I.; Garnett, E. C.; Shelton, S. W.; Fréchet, J. J. M.; Yang, P. Oligo- and polythiophene/ZnO hybrid nanowire solar cells. *Nano Lett.* **2010**, *10*, 334−340.
(16) Liu, J.; Tanaka, T.; Sivula, K.; Alivisatos, A. P.; Fréchet, J. M. J. Employing End-Functional Polythiophene To Control the Morphology of Nanocrystal-Polymer Composites in Hybrid Solar Cells. *J. Am. Chem. Soc.* **2004**, *126* (21), 6550−6551.
(17) McDonald, S. A.; Konstantatos, G.; Zhang, S.; Cyr, P. W.; Klem, E. J. D.; Levina, L.; Sargent, E. H. Solution-processed PbS quantum dot infrared photodetectors and photovoltaics. *Nat. Mater.* **2005**, *4* (2), 138−142.
(18) Cozzoli, P. D.; Kornowski, A.; Weller, H. Low-Temperature Synthesis of Soluble and Processable Organic-Capped Anatase TiO_2 Nanorods. *J. Am. Chem. Soc.* **2003**, *125* (47), 14539−14548.
(19) Lin, C.-C.; Ho, P.-H.; Huang, C.-L.; Du, C.-H.; Yu, C.-C.; Chen, H.-L.; Yeh, Y.-C.; Li, S.-S.; Lee, C.-K.; Pao, C.-W.; Chang, C.-P.; Chu, M.-W.; Chen, C.-W. Dependence of Nanocrystal Dimensionality on the Polymer Nanomorphology, Anisotropic Optical Absorption, and Carrier Transport in P3HT:TiO_2 Bulk Heterojunctions. *J. Phys. Chem. C* **2012**, *116* (47), 25081−25088.
(20) van Hal, P. A.; Wienk, M. M.; Kroon, J. M.; Verhees, W. J. H.; Slooff, L. H.; van Gennip, W. J. H.; Jonkheijm, P.; Janssen, R. A. J. Photoinduced electron transfer and photovoltaic response of a MDMO-PPV:TiO_2 bulk-heterojunction. *Adv. Mater.* **2003**, *15* (2), 118−121.
(21) Zhao, L.; Lin, Z. Crafting Semiconductor Organic-Inorganic Nanocomposites *via* Placing Conjugated Polymers in Intimate Contact with Nanocrystals for Hybrid Solar Cells. *Adv. Mater.* **2012**, *24* (32), 4353−4368.
(22) Moule, A. J.; Chang, L.; Thambidurai, C.; Vidu, R.; Stroeve, P. Hybrid solar cells: Basic principles and the role of ligands. *J. Mater. Chem.* **2012**, *22* (6), 2351−2368.
(23) Paoprasert, P.; Spalenka, J. W.; Peterson, D. L.; Ruther, R. E.; Hamers, R. J.; Evans, P. G.; Gopalan, P. Grafting of poly(3-hexylthiophene) brushes on oxides using click chemistry. *J. Mater. Chem.* **2010**, *20* (13), 2651−2658.
(24) Boon, F.; Thomas, A.; Clavel, G.; Moerman, D.; De Winter, J.; Laurencin, D.; Coulembier, O.; Dubois, P.; Gerbaux, P.; Lazzaroni, R.; Richeter, S.; Mehdi, A.; Clément, S. Synthesis and characterization of carboxystyryl end-functionalized poly(3-hexylthiophene)/TiO_2 hybrids in view of photovoltaic applications. *Synth. Met.* **2012**, *162* (17−18), 1615−1622.
(25) Kango, S.; Kalia, S.; Celli, A.; Njuguna, J.; Habibi, Y.; Kumar, R. Surface modification of inorganic nanoparticles for development of organic−inorganic nanocomposites—A review. *Prog. Polym. Sci.* **2013**, *38* (8), 1232−1261.
(26) Marshall, N.; Sontag, S. K.; Locklin, J. Surface-initiated polymerization of conjugated polymers. *Chem. Commun. (Cambridge, U. K.)* **2011**, *47* (20), 5681−5689.
(27) Alonzi, M.; Lanari, D.; Marrochi, A.; Petrucci, C.; Vaccaro, L. Synthesis of polymeric semiconductors by a surface-initiated approach. *RSC Adv.* **2013**, *3* (46), 23909−23923.
(28) Yokoyama, A.; Miyakoshi, R.; Yokozawa, T. Chain-growth polymerization for poly(3-hexylthiophene) with a defined molecular weight and a low polydispersity. *Macromolecules* **2004**, *37* (4), 1169−1171.
(29) Sheina, E. E.; Liu, J.; Iovu, M. C.; Laird, D. W.; McCullough, R. D. Chain Growth Mechanism for Regioregular Nickel-Initiated Cross-Coupling Polymerizations. *Macromolecules* **2004**, *37* (10), 3526−3528.
(30) Sui, A.; Shi, X.; Wu, S.; Tian, H.; Geng, Y.; Wang, F. Controlled Synthesis of Polyfluorenes via Kumada Catalyst Transfer Polycondensation with $Ni(acac)_2$/dppp as the Catalyst. *Macromolecules* **2012**, *45* (13), 5436−5443.
(31) Stefan, M. C.; Javier, A. E.; Osaka, I.; McCullough, R. D. Grignard Metathesis Method (GRIM): Toward a Universal Method for the Synthesis of Conjugated Polymers. *Macromolecules* **2009**, *42* (1), 30−32.
(32) Wen, H.; Ge, Z.; Liu, Y.; Yokozawa, T.; Lu, L.; Ouyang, X.; Tan, Z. Efficient synthesis of well-defined polycarbazoles via catalyst-transfer Kumada coupling polymerization. *Eur. Polym. J.* **2013**, *49* (11), 3740−3743.
(33) Yokozawa, T.; Ohta, Y. Scope of controlled synthesis via chain-growth condensation polymerization: from aromatic polyamides to π-conjugated polymers. *Chem. Commun. (Cambridge, U. K.)* **2013**, *49* (75), 8281−8310.
(34) Stefan, M. C.; Bhatt, M. P.; Sista, P.; Magurudeniya, H. D. Grignard metathesis (GRIM) polymerization for the synthesis of conjugated block copolymers containing regioregular poly(3-hexylthiophene). *Polym. Chem.* **2012**, *3* (7), 1693−1701.
(35) Senkovskyy, V.; Khanduyeva, N.; Komber, H.; Oertel, U.; Stamm, M.; Kuckling, D.; Kiriy, A. Conductive Polymer Brushes of Regioregular Head-to-Tail Poly(3-alkylthiophenes) via Catalyst-Transfer Surface-Initiated Polycondensation. *J. Am. Chem. Soc.* **2007**, *129* (20), 6626.
(36) Khanduyeya, N.; Senkovskyy, V.; Beryozkina, T.; Horecha, M.; Stamm, M.; Uhrich, C.; Riede, M.; Leo, K.; Kiriy, A. Surface Engineering Using Kumada Catalyst-Transfer Polycondensation (KCTP): Preparation and Structuring of Poly(3-hexylthiophene)-Based Graft Copolymer Brushes. *J. Am. Chem. Soc.* **2009**, *131* (1), 153−161.
(37) Senkosvskyy, V.; Tkachov, R.; Beryozkian, T.; Komber, H.; Oertel, U.; Horecha, M.; Bocharova, V.; Stamm, M.; Gervogyan, S. A.; Krebs, F.; Kiriy, A. "Hairy" poly(3-hexylthiophene) particles prepared via surface-initiated Kumada catalyst-transfer polycondensation. *J. Am. Chem. Soc.* **2009**, *131* (45), 16445−16453.
(38) Tkachov, R.; Senkovskyy, V.; Horecha, M.; Oertel, U.; Stamm, M.; Kiriy, A. Surface-initiated Kumada catalyst-transfer polycondensation of poly(9,9-dioctylfluorene) from organosilica particles: chain-confinement promoted β-phase formation. *Chem. Commun. (Cambridge, U. K.)* **2010**, *46* (9), 1425−1427.
(39) Bonhomme, C.; Gervais, C.; Laurencin, D. Recent NMR developments applied to organic-inorganic materials. *Prog. Nucl. Magn. Reson. Spectrosc.* **2014**, *77*, 1−48.
(40) Widdifield, C. M.; Cavallo, G.; Facey, G. A.; Pilati, T.; Lin, J.; Metrangolo, P.; Resnati, G.; Bryce, D. L. Multinuclear Solid-State Magnetic Resonance as a Sensitive Probe of Structural Changes upon the Occurrence of Halogen Bonding in Co-crystals. *Chem.—Eur. J.* **2013**, *19* (36), 11949−11962.
(41) Negishi, E. Palladium- or nickel-catalyzed cross coupling. A new selective method for carbon-carbon bond formation. *Acc. Chem. Res.* **1982**, *15* (11), 340−348.

(42) Yang, L.; Sontag, S. K.; LaJoie, T. W.; Li, W.; Huddleston, N. E.; Locklin, J.; You, W. Surface-Initiated Poly(3-methylthiophene) as a Hole-Transport Layer for Polymer Solar Cells with High Performance. *ACS Appl. Mater. Interfaces* **2012**, *4*, 5069−5073.
(43) Sontag, S. K.; Marshall, N.; Locklin, J. Formation of conjugated polymer brushes by surface-initiated catalyst-transfer polycondensation. *Chem. Commun. (Cambridge, U. K.)* **2009**, *23*, 3354−3356.
(44) Oosterbaan, W. D.; Vrindts, V.; Berson, S.; Guillerez, S.; Douheret, O.; Ruttens, B.; D'Haen, J.; Adriaensens, P.; Manca, J.; Lutsen, L.; Vanderzande, D. Efficient formation, isolation and characterization of poly(3-alkylthiophene) nanofibres: Probing order as a function of side-chain length. *J. Mater. Chem.* **2009**, *19* (30), 5424−5435.
(45) Le Bouch, N.; Auger, M.; Leclerc, M. Structure and segmental motions in a substituted polythiophene: a solid-state NMR study. *Macromol. Chem. Phys.* **2008**, *209* (24), 2455−2462.
(46) Bolognesi, A.; Porzio, W.; Provasoli, A.; Botta, C.; Comotti, A.; Sozzani, P.; Simonutti, R. Structural and thermal behavior of poly(3-octylthiophene): A DSC, ^{13}C MAS NMR, XRD, photoluminescence, and Raman scattering study. *Macromol. Chem. Phys.* **2001**, *202* (12), 2586−2591.
(47) Sundberg, M.; Inganäs, O.; Stafström, S.; Gustafsson, G.; Sjögren, B. Optical absorption of poly(3-alkylthiophenes) at low temperatures. *Solid State Commun.* **1989**, *71* (6), 435−439.
(48) Lu, S.; Zeng, L.; Wu, T.; Ren, B.; Niu, J.; Liu, H.; Zhao, X.; Mao, J. Efficient hybrid carboxylated polythiophene/nanocrystalline TiO_2 heterojunction solar cells. *Sol. Energy* **2011**, *85* (9), 1967−1971.
(49) Chen, C.-T.; Hsu, F.-C.; Sung, Y.-M.; Liao, H.-C.; Yen, W.-C.; Su, W.-F.; Chen, Y.-F. Effects of metal-free conjugated oligomer as a surface modifier in hybrid polymer/ZnO solar cells. *Sol. Energy Mater. Sol. Cells* **2012**, *107*, 69−74.
(50) Mena-Osteriz, E.; Meyer, A.; Langeveld-Voss, B. M. W.; Janssen, R. A. J.; Meijer, E. W.; Bäuerle, P. Two-Dimensional Crystals of Poly(3-Alkylthiophene)s: Direct Visualization of Polymer Folds in Submolecular Resolution. *Angew. Chem., Int. Ed.* **2000**, *39* (15), 2679−2684.
(51) Brinkmann, M.; Wittman, J. C. Orientation of regioregular poly(3-hexylthiophene) by directional solidification: a simple method to reveal the semicrystalline structure of a conjugated polymer. *Adv. Mater.* **2006**, *18* (7), 860−863.
(52) Qiao, Q.; Su, L.; Beck, J.; McLeskey, J. J. T. Characteristics of water-soluble polythiophene: TiO_2 composite and its application in photovoltaics. *J. Appl. Phys.* **2005**, *98* (9), 094906/1−094906/7.
(53) Liu, J.; Tanaka, T.; Sivula, K.; Alivisatos, A. P.; Fréchet, J. M. J. Employing End-Functional Polythiophene To Control the Morphology of Nanocrystal-Polymer Composites in Hybrid Solar Cells. *J. Am. Chem. Soc.* **2004**, *126* (21), 6550−6551.
(54) Xu, T.; Yan, M.; Hoefelmeyer, J. D.; Qiao, Q. Exciton migration and charge transfer in chemically linked P3HT-TiO_2 nanorod composite. *RSC Adv.* **2012**, *2* (3), 854−862.
(55) Liu, Y.; Scully, S. R.; McGehee, M. D.; Liu, J.; Luscombe, C. K.; Fréchet, J. M. J.; Shaheen, S. E.; Ginley, D. S. Dependence of band offset and open-circuit voltage on the interfacial interaction between TiO_2 and carboxylated polythiophenes. *J. Phys. Chem. B* **2006**, *110* (7), 3257−3261.
(56) Boon, F.; Desbief, S.; Cutaia, L.; Douhéret, O.; Minoia, A.; Ruelle, B.; Clément, S.; Coulembier, O.; Cornil, J.; Dubois, P.; Lazzaroni, R. Synthesis and Characterization of Nanocomposites Based on Functional Regioregular Poly(3-hexylthiophene) and Multiwall Carbon Nanotubes. *Macromol. Rapid Commun.* **2010**, *31* (16), 1427−1434.
(57) Pazokifard, S.; Mirabedini, S. M.; Esfandeh, M.; Mohseni, M.; Ranjbar, Z. Silane grafting of TiO_2 nanoparticles:dispersibility and photoactivity in aqueous solutions. *Surf. Interface Anal.* **2012**, *44*, 41−47.